Cloud Remote Sensing Using ARM Instruments: Observations and Modeling

M. Ovtchinnikov and Y. L. Kogan
Cooperative Institute for Mesoscale Meteorological Studies
Norman, Oklahoma

Introduction

The constantly expanding Atmospheric Radiation Measurement (ARM) instrumental base for observing clouds now consists of about a dozen instruments including ceilometers, lidars, and a cloud radar. The majority of these instruments provides indirect measurements and requires a use of retrieval algorithms to deduce cloud properties needed for developing and testing cloud parameterizations for general circulation models (GCMs). In situ aircraft measurements during intensive observation periods (IOPs) are intended to provide ground truth for testing these retrieval procedures. Unfortunately, aircraft sampling often is not complete enough for such tests. In this study, we are using a three-dimensional numerical cloud model with explicit microphysical parameterization to complement in situ measurements in supplying detailed information about cloud structure on a case study basis. This approach is particularly useful in the case of mixed-phase clouds for which fewer retrieval algorithms have been suggested and in situ measurements are less accurate than for all-liquid or all-ice clouds. In this paper, we present results from the April 7, 1997, case study and focus on the comparison of model results with direct microphysical observations.

Model

The model used in this study includes a three-dimensional dynamical framework coupled with explicit liquid and ice-phase microphysics based on prognostic equations for cloud drop and ice particle (IP) spectra. Each spectrum is represented by 28 bins covering the 2.7×10^{-10} to 3.6×10^{-2} gram mass range, which corresponds to 4 μm to 2.05 mm range in equivalent drop radii. The smallest 15 categories of IP are assumed to be plate-like crystals, while the largest 13 categories represent graupel particles. A separate distribution function for cloud condensation nuclei (CCN) contains 12 size categories. Microphysical processes for liquid and ice phases include nucleation, diffusional growth/evaporation, coalescence, and freezing/melting. The model accounts for all basic mechanisms of ice nucleation with separate parameterizations for the activation of immersion-freezing, deposition and condensation-freezing, and contact-freezing ice nuclei. To correctly describe the contact ice nucleation mode, a scavenging model is used to predict the collision rate for drop - ice nucleus interaction. In addition to the ice nucleation mechanisms, the model incorporates a parameterization of the Hallett-Mossop (H-M) rime-splintering mechanism. The splinter production rate is calculated based on the temperature and rate of graupel riming involving cloud droplets with diameters greater than 24 μm (Hallett and Mossop 1974). The riming rate is calculated explicitly by solving the stochastic collection equation for liquid drops and IP.

The computational domain covers $8 \times 8 \times 8$ km with a 250-meter spatial resolution in all directions. A 10-second time step is used in dynamical calculations, while a 0.2-second time step is used in microphysical calculations.

Case Study

During the day of April 7, 1997, a mixed-phase midlevel stratiform cloud layer formed over northern Oklahoma. The cloudiness persisted for several hours. During this period, the cloud layer was sampled by the Citation research aircraft of the University of North Dakota as well as by surface cloud observation instrumentation. The flight was part of the Cloud Radar IOP conducted under the ARM Program. The obtained data sets provide a wealth of information for testing and developing cloud retrieval algorithms for various combinations of remote sensing devices used by the ARM Program. The environmental soundings for the day are available from balloons that were launched from the Southern Great Plains (SGP) Central Facility approximately every 3 hours. The sounding used to initialize the model corresponds to 1730 UTC and is shown in Figure 1. There is a prominent, nearly saturated layer between 700 mb (~2.75 km) and 550 mb (~4.5 km) with a lapse rate that is almost moist adiabatic. The layer is capped by a drier and more stable layer above 4.5 km. The lower troposphere is also dry with relative humidity around 40%. The boundary layer is separated from the free atmosphere by an inversion

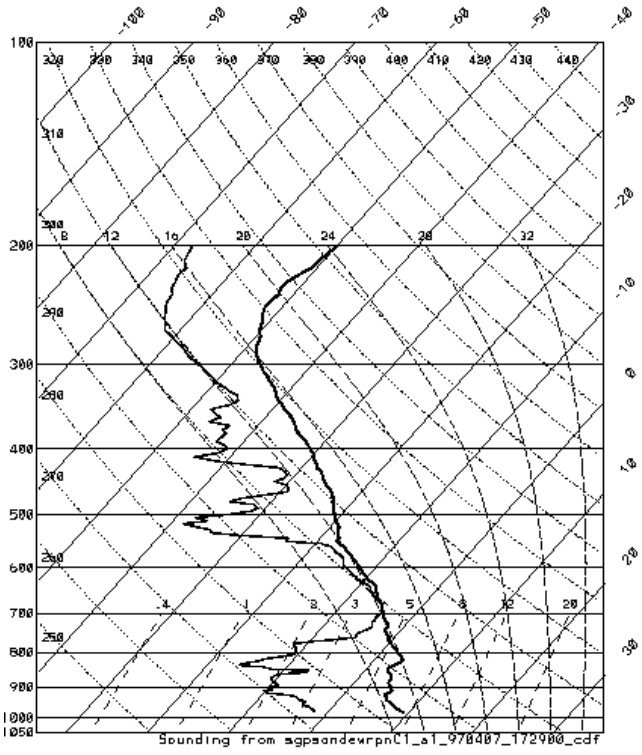

Figure 1. Skew T - log P diagram of environmental conditions for 1730 UTC April 7, 1997.

at 1.5 km. At the beginning of the integration, a saturated layer is specified between 3 km and 4 km. Random temperature perturbations of small amplitude (a few tenths of a degree) are used to send the layer in motion.

Aerosol properties were measured between 1900 and 2030 UTC by instrumentation onboard the Gulfstream-1 research aircraft. By that time clouds practically disappeared and most of the flight was under clear-sky conditions.

The vertical profile of the total aerosol concentration in the 0.11 μm to 2.75 μm size range is shown in Figure 2. Note that the inversion layer prevents high aerosol concentrations in the boundary layer from penetrating into the middle troposphere. The microstructure of the cloud, which was above 2.5 km, was not affected by the polluted boundary layer. In order to obtain the aerosol size spectrum representative of the cloud layer, we averaged data over all flight legs flown at or near 2.6 km. The resultant spectrum is shown in Figure 3. To a good approximation, all aerosol particles in the size range shown in Figure 3 act as CCN. Thus, the same spectrum was used to describe the initial CCN size distribution in the model.

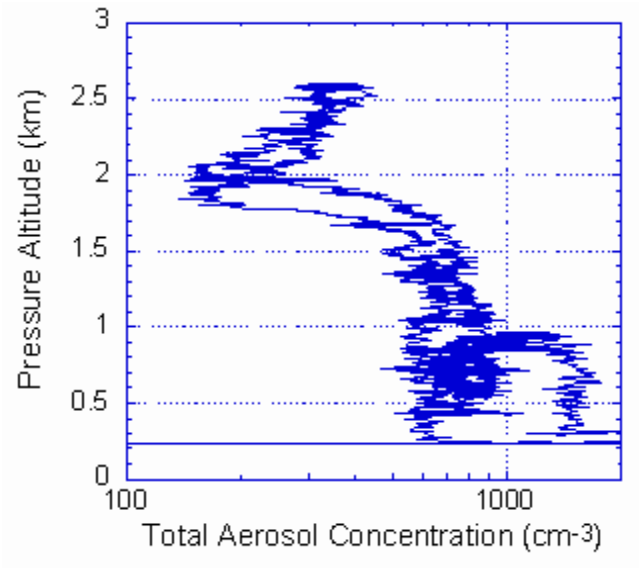

Figure 2. Total concentration of aerosol particles in a 0.11 μm to 2.75 μm size range measured by the PCASP as a function of height. The data are from the 1900 to 2030 UTC flight of the Gulfstream-1 research aircraft on April 7, 1997. (For a color version of this figure, please see *http://www.arm.gov/docs/documents/technical/conf_9803/ovtchinnikov-98.pdf.*)

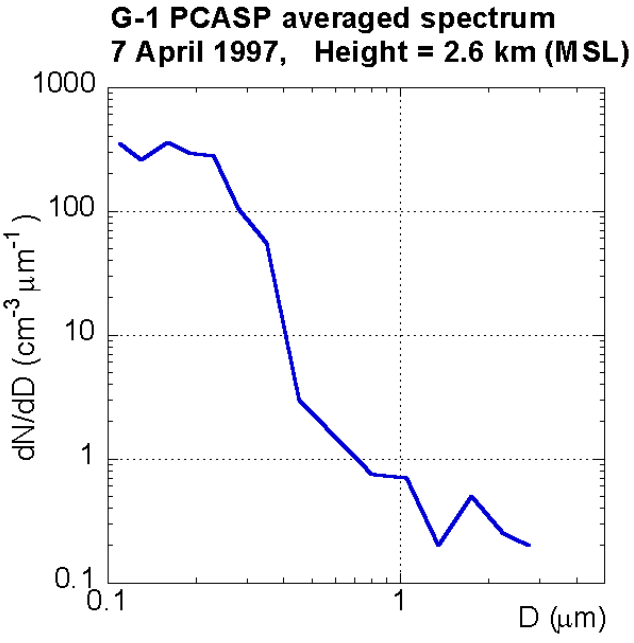

Figure 3. Size distribution of aerosol particles at 2.6 m on April 7, 1998. (For a color version of this figure, please see *http://www.arm.gov/docs/documents/technical/conf_9803/ovtchinnikov-98.pdf.*)

Results

Figure 4 outlines the vertical structure of the simulated cloud. The cloud base is rather flat except for the regions where drizzle or small raindrops are falling out. The upper part of the cloud layer is much more variable. Individual turrets are rising to a height of 5 km from a much more horizontal uniform cloud layer near 3 km. Similar structure is seen in the field of total cloud droplet concentration (Figure 5). Although the simulation corresponds to overcast conditions, both the liquid water content (LWC) and drop concentration fields are highly variable.

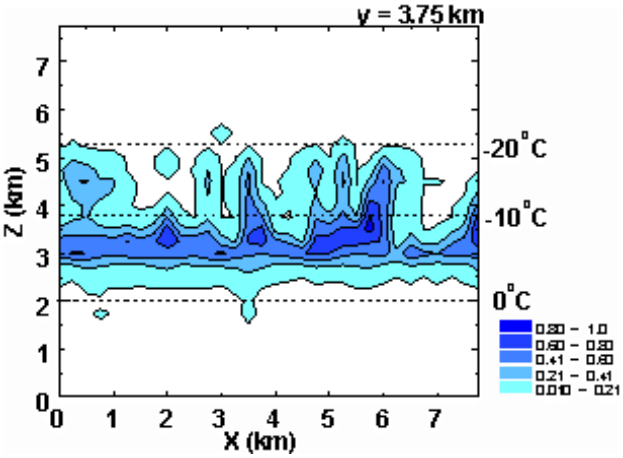

Figure 4. Vertical cross section of the LWC in (g m^{-3}). (For a color version of this figure, please see *http://www.arm.gov/docs/documents/technical/conf_9803/ovtchinnikov-98.pdf.*)

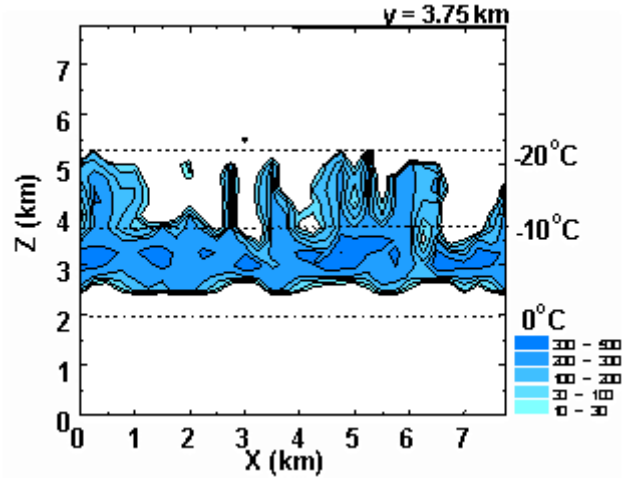

Figure 5. Vertical cross section of the cloud drop concentration in (cm^{-3}). (For a color version of this figure, please see *http://www.arm.gov/docs/documents/technical/conf_9803/ovtchinnikov-98.pdf.)*

The simulated structure of the cloud layer is supported by the in situ measurements taken by the Citation aircraft of the University of North Dakota. Figure 6 shows cloud droplet concentration measured by the Forward Scattering Spectrometer Probe (FSSP) at three different levels within the cloud layer. Lower-level penetration shows nearly solid cloud deck (Figure 6c) with averaged droplet concentration around 200 cm^{-3}. At higher altitudes, the cloud field is broken (Figure 6a).

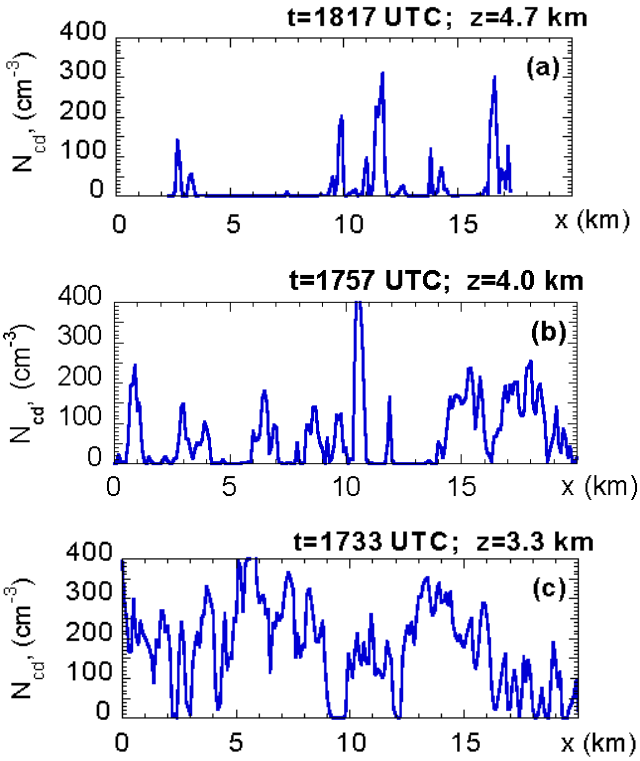

Figure 6. Total concentration of cloud drops as measured by the FSSP during three flight legs at various heights. The height and time of the beginning of each leg is indicated. (For a color version of this figure, please see *http://www.arm.gov/docs/documents/technical/conf_9803/ovtchinnikov-98.pdf.*)

Although aircraft instrumentation did not register any cloud or precipitation particles below 2.5 km, radar image of the cloud layer extends well below 2.0 km (Figure 7). This is due to drizzle, raindrops, and large ice particles that are present below cloud base defined in terms of LWC or cloud droplet concentration in Figures 4 and 5, respectively. Although the concentration of such particles is near or below a threshold for detection by aircraft instrumentation, their reflectivity is still comparable to the reflectivity of the cloud.

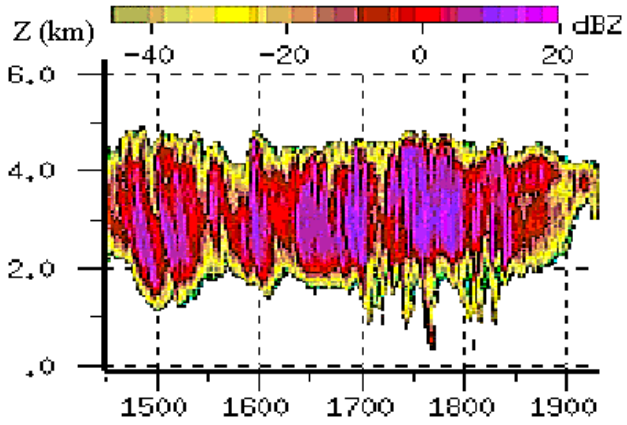

Figure 7. Time - height plot of the reflectivity factor from the millimeter-wavelength cloud radar (MMCR). (For a color version of this figure, please see *http://www.arm.gov/docs/documents/technical/conf_9803/ovtchinnikov-98.pdf.*)

Using cloud drop spectra provided by the model, we calculate radar reflectivity and extinction coefficient of the simulated cloud. One of the main goals of the ARM cloud observing instruments is to provide information about vertical and horizontal cloud distribution. This can be characterized by a vertical profile of the fractional cloud cover that at each level shows the fraction of the area occupied by cloud. The fractional cloud cover depends on the parameter used to define the cloud boundary and on the threshold value of this parameter. Figure 8 shows vertical profiles of fractional cloud cover for three parameters: LWC, extinction coefficient, and radar reflectivity factor. In terms of LWC, the cloud has a sharp cloud base, as was seen in Figure 4. In terms of the reflectivity factor, the cloud base height has much greater horizontal variability, which is in agreement with MMCR measurements (Figure 7). The difference between the various predictions of cloud geometry is stronger when drizzle or precipitation is present. This was the case on April 7, 1998, although precipitation hardly ever reached the ground.

Conclusions

A cloud model is used to simulate a stratiform cloud layer that formed over the SGP Cloud and Radiation Testbed (CART) site on April 7, 1998. Model predictions of the cloud geometry, LWC, cloud droplet concentration and ice particle concentration agree well with in situ aircraft measurements. Simulated three-dimensional detailed microphysical characteristics from the model are used to simulate return signals for various remote-sensing instruments. These are used to derive vertical profiles of fractional cloud cover. It is shown that even the most basic cloud parameters, such as the cloud base height or cloud thickness, are determined differently by various instruments, especially for clouds containing precipitating particles.

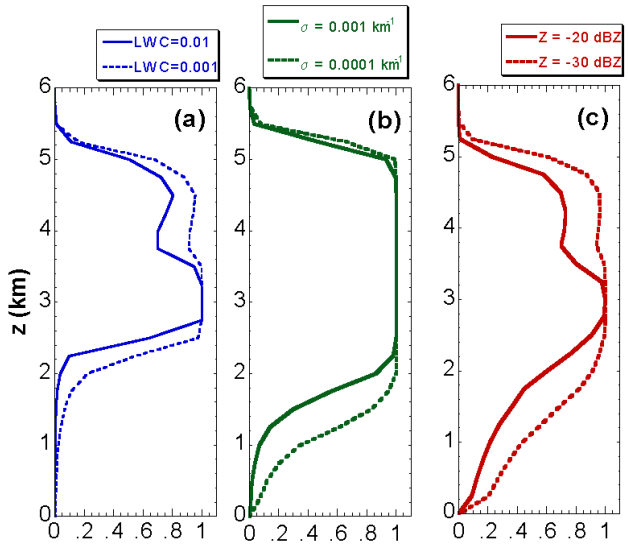

Figure 8. Fractional cloud cover versus height. Cloud boundary is defined in terms of liquid water content (a), extinction coefficient (b), and reflectivity factor (c). Threshold values separating cloudy and cloud-free points are indicated. (For a color version of this figure, please see *http://www.arm.gov/docs/documents/technical/conf_9803/ovtchinnikov-98.pdf.*)

Acknowledgments

This research was supported by the Environmental Sciences Division of the U.S. Department of Energy [through Battelle PNNL Contract 144880-A-Q1 to the Cooperative Institute of Mesoscale and Meteorological Studies (CIMMS)] as part of the ARM Program and by ONR Grant N00014-96-1-0687. The aircraft measurements were supplied by Mike Poellot of the University of North Dakota and by Pete Daum of Brookhaven National Laboratory.

Reference

Hallett, J., and S. C. Mossop, 1974: Production of secondary ice crystals during the riming process. *Nature*, **249**, 26-28.